applied sciences

MDPI

Article

A Transferable Prediction Approach for the Remaining Useful Life of Lithium-Ion Batteries Based on Small Samples

Haochen Qin, Xuexin Fan, Yaxiang Fan *, Ruitian Wang, Qianyi Shang and Dong Zhang

National Key Laboratory of Electromagnetic Energy, Naval University of Engineering, Wuhan 430033, China; qin_mail2022@163.com (H.Q.)
* Correspondence: fanyaxiang_1989@163.com

Abstract: Predicting the remaining useful life (RUL) of batteries can help users optimize battery management strategies for better usage planning. However, the RUL prediction accuracy of lithium-ion batteries will face challenges due to fewer data samples available for the new type of battery. This paper proposed a transferable prediction approach for the RUL of lithium-ion batteries based on small samples to reduce time in preparing battery aging data and improve prediction accuracy. This approach, based on improvements from the adaptive boosting algorithm, is called regression tree transfer adaptive boosting (RT-TrAdaBoost). It combines the advantages of ensemble learning and transfer learning and achieves high computational efficiency. The RT-TrAdaBoost approach takes the charging voltage and temperature curve as input and utilizes the classification and regression tree (CART) as the base learner, which has better feature capture ability. In the experiment, the working condition migration experiment and battery type migration experiment are conducted on non-overlapping datasets. The verified results revealed that the RT-TrAdaBoost approach could transfer not only the battery aging knowledge between various working conditions but also realize the RUL migration prediction from lithium iron phosphate battery to lithium cobalt oxide battery. The analysis of error and computation time demonstrates the proposed method's high efficiency and speed.

Keywords: lithium-ion battery; remaining useful life; transfer adaptive boosting; CART; battery management system; edge computing

Citation: Qin, H.; Fan, X.; Fan, Y.; Wang, R.; Shang, Q.; Zhang, D. A Transferable Prediction Approach for the Remaining Useful Life of Lithium-Ion Batteries Based on Small Samples. *Appl. Sci.* **2023**, *13*, 8498. https://doi.org/10.3390/app13148498

Academic Editor: Young-Kyu Han

Received: 29 June 2023
Revised: 20 July 2023
Accepted: 21 July 2023
Published: 23 July 2023

1. Introduction

Renewable energy is gradually becoming an important option to replace fossil energy [1]. As one of the most popular renewable energy storage solutions, lithium-ion batteries have the advantages of high energy density, long cycle life, and low pollution [2]. However, the lifespan of lithium-ion batteries will be reduced through recycling, and improper usage will expedite battery aging [3]. When the aging reaches a certain level, the lithium-ion battery will not work properly [4]. Therefore, lithium-ion batteries are often equipped with a battery management system (BMS) to accurately predict the remaining useful life (RUL) of the battery [5].

The RUL is one of the important indicators to measure the aging degree of lithium-ion batteries, and it is closely correlated with the state of health (SOH) of lithium-ion batteries [6]. When the SOH of lithium-ion batteries falls below a certain threshold, their operational performance will inevitably deteriorate [7]. This threshold is called the end-of-life (EOL), usually when SOH drops to 80% of the rated value [8,9]. The moment at which the SOH exceeds this threshold can be referred to as the end-of-monitoring (EOM). Therefore, the RUL is commonly defined as the total number of charge–discharge cycles a battery can undergo from the EOM to the EOL [10], expressed as follows

$$RUL = n_{EOL} - n_{EOM} \quad (1)$$

n_{EOL} is the number of cycles when the new battery cycles to the threshold, and n_{EOM} represents the current cycle number.

Recently, many methods have been proposed to solve the RUL prediction problem. These methods are primarily categorized as model-based methods and data-driven methods [11]. The model-based method primarily establishes the correlation between measurable physical parameters and the RUL by leveraging the electrochemical mechanism or circuit characteristics of lithium-ion batteries [12,13]. The literature [14] investigates an empirical exponential growth model for the resistance degradation of lithium-ion batteries, using particle filtering (PF) to evaluate aging data at different time intervals indicative of system health. The literature [15] explores the performance of different circuit topologies for diffusion processes. Although the aforementioned research has contributed to the study of remaining life prediction for lithium-ion batteries, developing an accurate battery model requires a significant amount of expertise [16]. Additionally, the RUL of lithium-ion batteries is not only limited by their aging mechanism but also closely linked to complex operating conditions and battery types [17]. When the battery's working environment is disturbed, the stability of the model will face challenges [18]. Therefore, model-based methods are often insufficiently flexible.

Based on the data-driven method to extract the aging law of lithium-ion batteries from battery aging data, it can be more flexibly adapted to online prediction [19]. It mainly includes the signal processing method, neural network method, and machine learning method [20]. The signal processing method usually summarizes the law from the time domain and frequency domain characteristics of the signal. In the literature [21], the empirical mode decomposition (EMD) method is adopted to decompose the capacity curve into linear and nonlinear trends, which is convenient for research separately. Unlike signal processing methods, neural network methods are often utilized in the form of enhancement or combination to predict the RUL of lithium-ion batteries. Literature [22] combined the convolutional neural network (CNN), the bidirectional long short-term memory (Bi-LSTM), and the Bayesian network to develop a Bayesian neural network (BNN). This method utilizes only a small amount of data to accurately predict the RUL of batteries. Literature [23] constructed the deep learning model based on bi-directional long short-term memory(Bi-LSTM) with the addition of an attention mechanism(AM) to focus on the important parts of the batteries' features. Additionally, the machine learning method is widely adopted for RUL prediction. The literature [24] analyzed the different characteristics of the early and long-term aging paths of lithium-ion batteries and utilized random logistic regression to classify batteries with different aging paths to perform accurate RUL predictions. The ensemble learning method is a kind of machine learning method that can embody collective intelligence and has the advantages of high calculation accuracy and low time cost [25]. It exhibits strong feature recognition capabilities, obviating the need for manual feature extraction and rendering it highly suitable for deployment in BMS applications aimed at predicting battery RUL. Ensemble learning techniques have been employed in studies aimed at addressing the problem of predicting RUL. Zhu et al. used the adaptive boosting (AdaBoost) algorithm to mine data features and fused it with LSTM to build a model to realize the RUL prediction of lithium-ion batteries [26]. The aforementioned study employs AdaBoost as a feature extraction approach, but it is not restricted to this, and the AdaBoost approach can also be used to construct prediction models directly [27]. In summary, the data-driven method offers advantages over the model-based method by avoiding establishing complex battery aging mechanism models and providing capabilities to solve nonlinear problems such as RUL prediction.

Typically, the data-driven approach necessitates a substantial volume of battery-related data to ensure the precision of the prediction [28]. However, the available samples of battery aging data for new-type batteries are typically limited in scale. Therefore, the limited data samples are insufficient to fully describe the entire degradation process of the battery. It will require a significant amount of time to gather adequate aging data for the tested battery. For instance, in the Oxford dataset on battery degradation, lithium iron phosphate

(LFP) batteries undergo cyclic charging and discharging at a rate of 1C until they reach the EOL. This entire process spans over 8000 cycles and lasts for nearly 300 days [29]. Hence, the utilization of data from pre-existing batteries for prognosticating novel battery types is being contemplated. Although the public datasets for lithium-ion batteries are abundant, the data on different types of batteries often fail to accurately reflect the nuances of aging between each other. Furthermore, the degradation of lithium-ion batteries varies under different operating conditions, posing challenges for accurate predictions in practical applications. Hence, it is crucial to establish a transferable predictive methodology for the remaining useful life (RUL) of lithium-ion batteries based on small data samples. This approach should effectively apply valuable information from historical data to a small number of battery samples under test, thereby significantly reducing the overall development cycle of the battery life prediction algorithm.

To accomplish the aforementioned objectives, transfer learning (TL) can be employed to facilitate the transfer of battery aging knowledge across disparate battery datasets. The contributor and receiver of the transfer are called the source domain and the target domain, respectively [30]. For lithium-ion batteries, there is a difference in the distribution between the source domain and the target domain due to different operating conditions or battery types, and this difference is called domain shift [31]. To solve the domain shift between different distribution datasets, literature [32] established a battery RUL prediction model using the migration method from the perspective of cycle consistency of degradation trend. Similarly, the literature [33] combined the particle filter and LSTM network and proposed a TL-LSTM-PF model with transfer learning ability, which better realized the transfer prediction between datasets of different charging conditions on the LFP battery. Although these studies have yielded favorable outcomes, there remain two aspects that require further investigation.

1. In some existing methods for predicting the RUL, there is a degree of data overlap between the source and target domains. However, in the actual situation, the target domain data reflects the aging degree of the new battery under the current working conditions. The source domain data are often from old batteries. Data between these two domains should not overlap. Although setting up experiments under partial overlap will reduce the difficulty of transfer learning and help to obtain better experimental results, it does not meet the needs of actual engineering.
2. RUL migration prediction is limited to the same type of battery under different working conditions and does not extend to migration between different types of batteries. To provide users with accurate battery life information, it often takes a lot of time to perform cycle aging experiments to predict the life of new battery models. However, this will delay the sale of new type battery, so data from older batteries with different materials can be considered for migration prediction. For example, the migration from LFP batteries aging data to lithium cobalt oxide (LCO) batteries aging data can be explored.

To address the aforementioned limitations, this paper proposes a transfer learning approach based on small sample sizes that leverages the strengths of both ensemble learning and transfer learning. The approach called regression tree transfer adaptive boosting (RT-TrAdaBoost) utilizes the directly measurable charging voltage and temperature as input variables, facilitating accurate prediction of the RUL of lithium-ion batteries. To enhance the ability to capture intrinsic features, we have innovatively employed classification and regression tree (CART) as the base learner of the RT-TrAdaBoost model for learning the mapping relationship between aging data and remaining life. Subsequently, non-overlapping target and source domains are created from the battery dataset, followed by conducting experiments under various working conditions and different types of batteries. Finally, the proposed approach is validated on both a personal computer and an edge intelligent computing module. Through analysis of errors and calculation times, it has been demonstrated that this approach is both fast and effective. The main contributions of this paper are summarized as follows:

1. To accurately transfer battery knowledge from historical data to small samples, this paper utilizes the advantages of ensemble learning and transfer learning to establish the RT-TrAdaBoost model for predicting the RUL of lithium-ion batteries.
2. Considering the deployment of the approach on BMS, the directly measurable charging voltage and temperature curves are used as the input of the model. Utilizing CART as the base learner of the established model improves the model's ability to capture battery data features.
3. This paper establishes non-overlapping target and source domains in order to make the research more practical. We not only evaluate the adaptability of the RT-TraAdaBoost model under varying working conditions for a single battery type but also investigate its transferability from LFP batteries to LCO batteries. The experimental results demonstrate satisfactory performance in terms of prediction accuracy and processing time.

The subsequent chapters are structured as follows: Section 2 introduces the proposed RUL prediction approach for lithium-ion batteries. Section 3 presents data preparation. Section 4 focuses on the analysis of the experimental results. Section 5 summarizes the conclusions drawn from this study.

2. Method for RUL Prediction

This section presents a lithium-ion battery RUL prediction model based on the RT-TrAdaBoost algorithm. It aims to transfer the knowledge of lithium-ion battery aging from historical data to small-scale samples of batteries under test. First, we formulate the RUL prediction problem. Then, the working principle of CART is introduced. Finally, the transfer learning framework is introduced based on AdaBoost. The CART-based learner is used to describe the mapping relationship between the battery aging data and the RUL, and the RT-TrAdaBoost model for predicting RUL is developed.

2.1. Problem Formulation

To enable transfer learning, we employ partially labeled training data with the same distribution as the test data to build an RUL prediction model. These data are called the same-distribution training data. When the size of the training data with the same distribution is insufficient, it becomes very difficult to train a precise battery aging mapping relationship for the test data. The training data whose distribution is different from that of the test data are called diff-distribution training data. Although these data are usually ample, their RUL prediction results on test data are often not ideal due to the different distribution. Specifically, let X_s be the same-distribution sample space, X_d the diff-distribution sample space, and S the label. The concept of battery aging is a function $f(\cdot)$ mapped from X to Y, where $X = X_s \cup X_d$, which can be expressed as follows

$$f(\bullet) : X \to Y,\ X = X_s \cup X_d \tag{2}$$

The test dataset is represented by $S = \{(x_i^t)\}$, where $x_i^t \in X_s (i = 1, \ldots, k)$. k is the size of the unlabeled testing set S. The training dataset $T \subseteq \{X \times Y\}$ is split into two labeled sets, T_{source} and T_{target}. T_{source} represents the $T_{source} = \left\{(x_i^d, c(x_i^d))\right\}$, where $x_i^d \in X_d (i = 1, \ldots, n)$. T_{target} is denoted by $T_{target} = \left\{(x_j^s, c(x_j^s))\right\}$, where $x_j^s \in X_s (i = 1, \ldots, m)$. m and n are the sizes of T_{target} and T_{source} separately. $c(x)$ is the label of the data sample x. The combined training set $T = \{(x_i, c(x_i))\}$ is expressed as follows

$$x_i = \begin{cases} x_i^d, & i = 1, \ldots, n \\ x_i^s, & i = n+1, \ldots, n+m \end{cases} \tag{3}$$

T_{source} corresponds to the source domain battery data, but it is unknown which part T_{source} is beneficial for training. Thus, utilizing T_{target} to find out the useful part of T_{source}, which is the running idea of the RT-TrAdaBoost algorithm. Therefore, given a small amount

of labeled training data T_{target} of the same distribution, training data T_{source} of a different distribution, and unlabeled test data S, the goal of RT-TrAdaBoost is to train a strong learner $\hat{f}(\bullet)$ such that the unlabeled data. The prediction error on the set S is minimum, which can be described as follows.

$$\begin{aligned} &min\left|\hat{f}(x_i) - c(x_i)\right| \\ &s.t.x_i \in X_s(i = 1, \ldots, k) \end{aligned} \tag{4}$$

2.2. CART

To enhance the feature capture ability of the model for battery aging data, this paper adopts CART as the base learner to depict the correlation between battery aging information and the RUL. The CART grows iteratively and can establish a nonlinear mapping on the given data [34]. Moreover, CART employs the principle of minimizing squared error to identify data features and grows into a binary decision tree by recursively splitting nodes based on prominent features in the data [35]. Randomly select the k-th variable $x^{(k)}$ of the feature data of the training set as the split variable, and the value s of this variable is used as the split point. The split point can divide the dataset into two regions R_1 and R_2:

$$R_1(k,s) = \left\{x \middle| x^{(k)} \le s\right\}, R_2(k,s) = \left\{x \middle| x^{(k)} \ge s\right\} \tag{5}$$

The output predictions c_1 and c_2 for each region are

$$c_m = \frac{1}{N_m}\sum\nolimits_{x_i \in R_m(k,s)} c_{im}(m = 1,2) \tag{6}$$

Among them, c_{im} is the optimal value of the i-th group of training data in the region m, and N_m indicates the amount of data in the region. Taking this as a comparison, the sum of squared errors in each area can be minimized by traversing the different values of k and s. The equation is as follows

$$L_{CART} = \min_{k,s}\left[\sum_{x_i \in R_1(k,s)} (c_{im} - c_1)^2 + \sum_{x_i \in R_2(k,s)} (c_{im} - c_2)^2\right] \tag{7}$$

where k and s are the best-split variables and split points. In subsequent splits, the above steps will be repeated until a complete decision tree is formed. The number of repetitions is related to the depth setting of the tree. In this paper, the maximum depth of CART is set to 5 layers, as shown in Figure 1. The resultant tree structure indicates a sequential arrangement of battery aging feature importance within the training dataset, serving as the base learner for RT-TrAdaBoost methodology and playing an essential role in predicting the RUL.

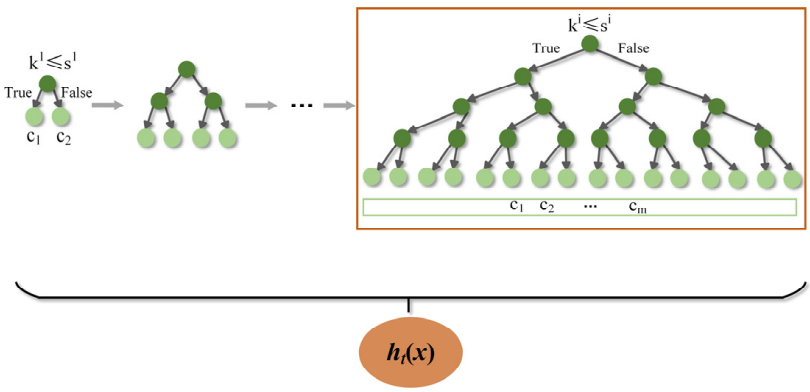

Figure 1. CART growth process.

2.3. AdaBoost Algorithm

AdaBoost is an ensemble learning algorithm based on boosting strategy [36]. First, it updates the weights of each sample through continuous iteration and trains to form a learner with preliminary capabilities. Then, through a weighted linear combination, each base learner is integrated into a strong learner with mature capabilities. Whether it is updating sample weights or weighting in ensembles, the AdaBoost can adapt to the training error rate to ensure that samples with lower error rates or base learners have higher weights. The principle of AdaBoost is briefly introduced below.

First, an initial weight vector is set such that each sample has an equal initial weight as follows.

$$w_i^t = \frac{1}{n} \quad 1 \le i \le n, t = 1 \tag{8}$$

Then, the base learner is used as a mapping h_t, which t represents the number of iterations. The map is trained with the training set T and weight vectors and validated on the testing set. Among all the test samples, the value d_t with the largest error is

$$d_t = \max_{i=1}^{n} |y_i - h_t(x_i)| \tag{9}$$

Since the key of AdaBoost is to redistribute weights to samples with large errors in the next iteration, the measurement of the error size should be compared with the largest error value in all samples. To describe the training error, the error needs to be normalized. Applying the exponential loss function, the adjusted error e_i^t of each instance is obtained as

$$e_i^t = 1 - exp\left(\frac{-|y_i - h_t(x_i)|}{d_t}\right) \tag{10}$$

In the case that the structure of the CART learner and the training set remains unchanged, the size of these adjustment errors changes with the change of the weight vector. Therefore, the sum of the product of the sample weights and the corresponding adjustment errors can be used to measure the predictive performance of the mapping. The resulting value is the total error of the mapping:

$$\varepsilon_t = \sum_{i=1}^{n} e_i^t w_i^t \tag{11}$$

In general, the probability of a random judgment error is 0.5. Therefore, when ε_t is greater than 0.5, the iteration will stop. Confidence for this error is usually defined β_t as follows:

$$\beta_t = \frac{\varepsilon_t}{1 - \varepsilon_t} \tag{12}$$

The lower the β_t is, the higher the reliability of the prediction made by the mapping. Utilize this value to update the sample weight vector as follows:

$$w_i^{t+1} = \frac{w_i^t \beta_t^{1-e_i^t}}{Z_t} \tag{13}$$

where Z_t represents the normalization constant, which ensures that its sum is still 1 after the weights are reassigned. The whole iterative process is shown in Equations (9)–(13). The smaller the loss produced by the sample x_i in t-th iteration, the lower the weight of the next iteration will be. As the number of iterations increases, the learners focus on samples with larger errors by increasing the weight.

The second weight adjustment occurs after the iteration stops, and all learners are weighted together. For a given input x_i, each learner will make a prediction and get the result $h_t(x_i)$. Finally, using $\ln(1/\beta_t)$ as weights, the weighted median of all learner results is the total prediction $h_f(x)$.

Despite its predictive capabilities, the Adaboost algorithm presupposes that all training data is distributed identically. However, differences in operating conditions or battery types can result in variations between the distribution of historical datasets and those to be tested, ultimately leading to a decrease in RUL prediction accuracy.

2.4. RT-TrAdaBoost Model

To solve the problem of low prediction accuracy, this section performs migration improvement based on the AdaBoost algorithm and develops the RT-TrAdaBoost model based on the CART-based learner. The model predicts lithium-ion battery RUL using only minimal data samples of the battery under test. It can effectively transfer the concept of lithium-ion battery aging in different distributed datasets from the historical battery dataset to the dataset under test, and its principle is illustrated in Figure 2.

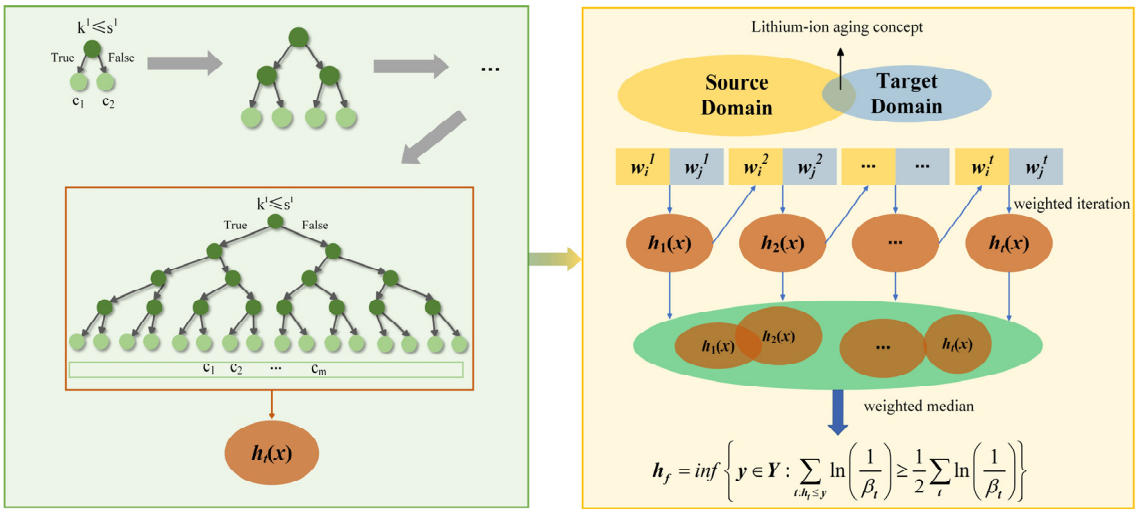

Figure 2. Principle of RT-TrAdaBoost approach.

Compared with the AdaBoost algorithm, the improvement of the RT-TrAdaBoost algorithm mainly reflects two aspects. One is to embed CART as a base learner into the algorithm, and the other is to treat the battery samples used for training unequally. Specifically, the weight vector produced by the t-th iteration is first normalized by

$$p^t = \frac{w^t}{\sum_{i=1}^{n+m} w_i^t} \tag{14}$$

Use the combined training set T mentioned in Section 2.1 and the standardized weight p^t generated by the t-th iteration to train on CART to obtain the mapping between battery aging information and RUL. The mapping is validated on the testing set, and the prediction error is calculated. The maximum value is

$$D_t = \max_{i=1}^{n} |c(x_i) - h_t(x_i)| \tag{15}$$

The error is also adjusted using the exponential loss function in the same way as Equation (10). The adjusted error reflects the predictive power of the mapping for each sample on the testing set. Then, to evaluate the effect of the current round of iteration and adjust the weight of the next iteration, the sum of these errors is calculated.

$$\varepsilon_t = \sum_{i=n+1}^{n+m} \frac{w_i^t \cdot e_i^t}{\sum_{i=n+1}^{n+m} w_i^t} \tag{16}$$

Compared with the AdaBoost approach, the RT-TrAdaBoost does not include the source domain data T_{source} when calculating the sum of errors. It aims to make the target domain data T_{target} with the same distribution as the testing sets play a greater role in training. Likewise, Equation (12) is used to calculate the confidence of this part of the sum of errors. For the source domain data, fixed confidence is used as follows:

$$\beta = \frac{1}{1+\sqrt{\frac{2\ln n}{N}}} \tag{17}$$

Then, the new weight vector in the next iteration is updated with Equation (18).

$$w_i^t = \begin{cases} w_i^t \beta^{e_i^t}, & 1 \le i \le n \\ w_i^t \beta_t^{-e_i^t}, & n+1 \le i \le n+m \end{cases} \tag{18}$$

The updated weights are, in turn, normalized by Equation (12). In this way, samples in the target domain and samples with smaller prediction errors in the source domain will get greater weights. For some samples with large prediction errors in the source domain, the weight will gradually decrease. After multiple iterations, the battery aging information in the source domain will gradually migrate to the target domain. Finally, by taking the weighted median of all the mapping sets produced by iterations, the expression is

$$h_f = \inf\left\{ y \in Y : \sum_{t:h_f \le y} \ln\left(\frac{1}{\beta_t}\right) \ge \frac{1}{2}\sum_t \ln\left(\frac{1}{\beta_t}\right) \right\} \tag{19}$$

h_f represents the final mapping result. The pseudocode of the RT-TrAdaBoost is given, as shown in Algorithm 1. According to Algorithm 1, if the prediction results of diff-distribution training samples significantly deviate from the actual values in each iteration round, it suggests that these samples may differ greatly from those in the same-distribution training data set and thus fail to accurately reflect battery aging details. Therefore, it is necessary to decrease its weight during training in order to mitigate its impact on the subsequent iteration. The weights of these diff-distribution training samples gradually diverge from those of the same-distribution battery samples. After sufficient iterations, the diff-distribution training weight of samples that better fit the same-distribution will be increased, while those that are dissimilar to the same-distribution training samples can only obtain lower weights. This process is the key component for achieving accurate battery RUL prediction using the proposed method. The flowchart of the entire proposed method is depicted in Figure 3.

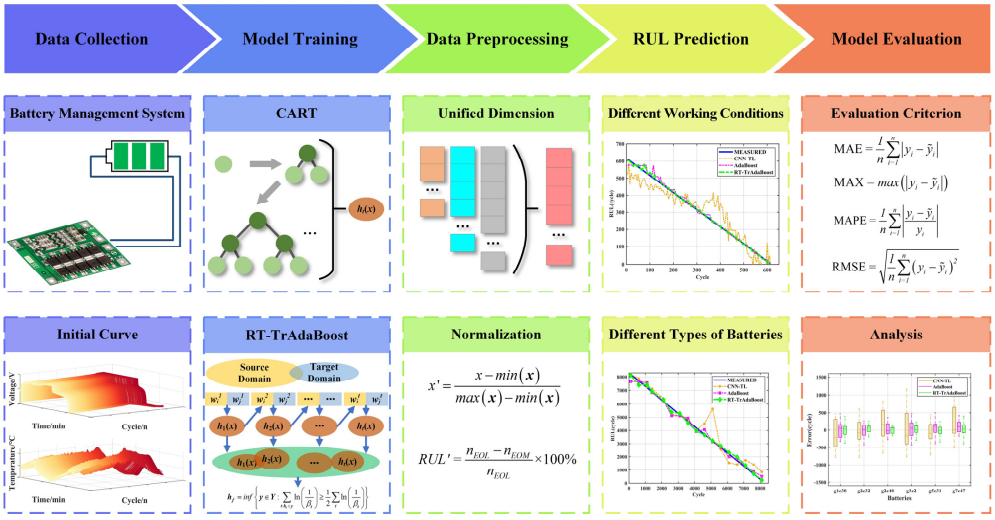

Figure 3. Workflow of the transferable lithium-ion batteries RUL prediction based on small samples.

Algorithm 1. Training algorithm for estimating the RUL

Input unlabeled dataset S

Data The combined sample set T consisting of both T_{source} and T_{target}

1 Initialize the weight vector w_i^1

For $t = 1, \ldots, N$:

2 Set normalized weight vector p^t

3 Use the combined training set T and the t-th iteration normalized weight vector p^t to train on the base learner CART to obtain the hypothesized mapping h_t. Enter S to get the label.

4 Compute the adjusted error e_i^t for the label of each sample on S the:

$$\text{let } D_t = \max_{i=1}^{n} |c(x_i) - h_t(x_i)|$$
$$\text{then } e_i^t = 1 - exp(-|c(x_i) - h_t(x_i)|/D_t)$$

5 Compute the total adjusted error of h_t on T_{target}:

$$\varepsilon_t = \sum_{i=n+1}^{n+m} \frac{w_i^t \cdot e_i^t}{\sum_{i=n+1}^{n+m} w_i^t}$$

6 Let $\beta_t = \varepsilon_t/(1-\varepsilon_t)$ and $\beta = 1/(1+\sqrt{2\ln n/N})$. Once the value is greater than 0.5, stop iterating.

7 Update the new weight vector:

$$w_i^{t+1} = \begin{cases} w_i^t \beta^{e_i^t}, & 1 \le i \le n \\ w_i^t \beta_t^{-e_i^t}, & n+1 \le i \le n+m \end{cases}$$

Output $y = h_f(x)$ is the weighted median of all mapping results $h_t(x)$, $t \in (1, N)$, and the mapping weight is $\ln(1/\beta_t)$

3. Data Preparation

3.1. Experimental Dataset

3.1.1. Stanford–MIT–Toyota Dataset

Attia et al. publicly released the Stanford–MIT–Toyota dataset, which utilized LFP batteries manufactured by A123 Systems [37]. The information on the battery is shown in Table 1.

Table 1. The information of battery in Stanford–MIT–Toyota dataset.

Stanford–MIT–Toyota Dataset	
Manufacturers	A123 Systems (APR18650M1A)
Battery Type	$LiFeO_4$
Nominal Capacity	1.1 Ah
Nominal Voltage	3.3 V
Charging Upper Limit Voltage	3.6 V
Discharging Termination voltage	2.0 V

The cells in this dataset were subjected to cycle charge and discharge experiments at a constant temperature of 30 degrees Celsius. The charging profile used was called the six-step fast charging mode. The first four steps of charging were all charged by constant current, and the total time was fixed at 10 min. The charging current was independently and randomly set in the four stages of battery SOC of 0–20%, 20–40%, 40–60%, and greater than 60%. The charging mode of the last two steps of all cells was the constant current and constant voltage (CCCV) under 1C. This paper selects the fifth batch of the dataset for research. This batch contains 9 different working conditions and a total of 45 batteries. All cells are still named according to their working condition type and channel number. For example, the cell tested in the 38th channel of the first working condition is called g1c38, and its voltage and temperature curves are shown in Figure 4. The corresponding details of working conditions and cell numbers are illustrated in Table 2.

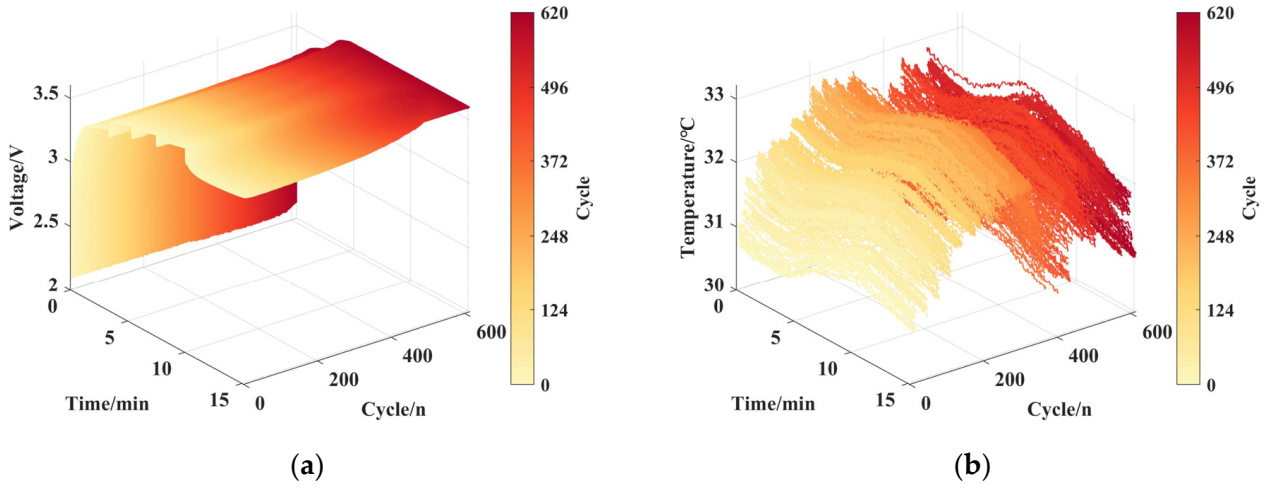

Figure 4. Charging curve of g1c38. (**a**) Voltage. (**b**) Temperature.

Table 2. The working condition of the battery in the Stanford–MIT–Toyota dataset.

Number	The First Four Steps	Cell Number
1	3.6A → 6A → 5.6A → 4.755A	g1c11, g1c12, g1c27, g1c29, g1c38
2	4.4A → 5.6A → 5.2A → 4.252A	g2c8, g2c15, g2c18, g2c32, g2c48
3	4.8A → 5.2A → 5.2A → 4.16A	g3c1, g3c2, g3c10, g3c20, g3c42
4	5.2A → 5.2A → 4.8A → 4.16A	g4c6, g4c7, g4c37, g4c41, g4c45
5	6A → 5.6A → 4.4A → 3.834A	g5c9, g5c21, g5c22, g5c31, g5c36
6	7A → 4.8A → 4.8A → 3.652A	g6c3, g6c25, g6c26, g6c28, g6c44
7	8A → 4.4A → 4.4A → 3.94A	g7c13, g7c16, g7c23, g7c24, g7c47
8	8A → 6A → 4.8A → 3A	g8c14, g8c17, g8c30, g8c35, g8c39
9	8A → 7A → 5.2A → 2.68A	g9c19, g9c33, g9c34, g9c40, g9c43

3.1.2. Oxford Battery Degradation Dataset

The Oxford Battery Degradation Dataset (Hereinafter referred to as the Oxford dataset) was released by Birkl et al. using the SLPB533459H4 LCO battery manufactured by Kokam. The rated capacity of this battery is 740 mAh [29]. The specifications of the battery are shown in Table 3.

Table 3. The specifications of battery in Oxford dataset.

Oxford Battery Degradation Dataset	
Manufacturers	Kokam (SLPB533459H4)
Battery Type	$LiCoO_2$
Nominal Capacity	740 mAh
Nominal Voltage	3.7 V
Charging Upper Limit Voltage	4.2 V
Discharging termination voltage	2.7 V

The dataset includes a total of 8 batteries, which were placed on the Bio-Logic MPG-205 battery test equipment. These cells were tested in a thermal chamber at 40 degrees Celsius. The charging strategy adopted the CCCV, and the discharge mode was constant current discharge to cut-off voltage. It is worth noting that this dataset only includes the constant-current charge and constant-current discharge stages of the battery charging process, both at 1C current. Therefore, this dataset does not capture current data. The eight cells in the Oxford dataset are named Cell1 to Cell8 in sequence. Taking Cell7 as an example, the charging voltage and temperature curves are shown in Figure 5.

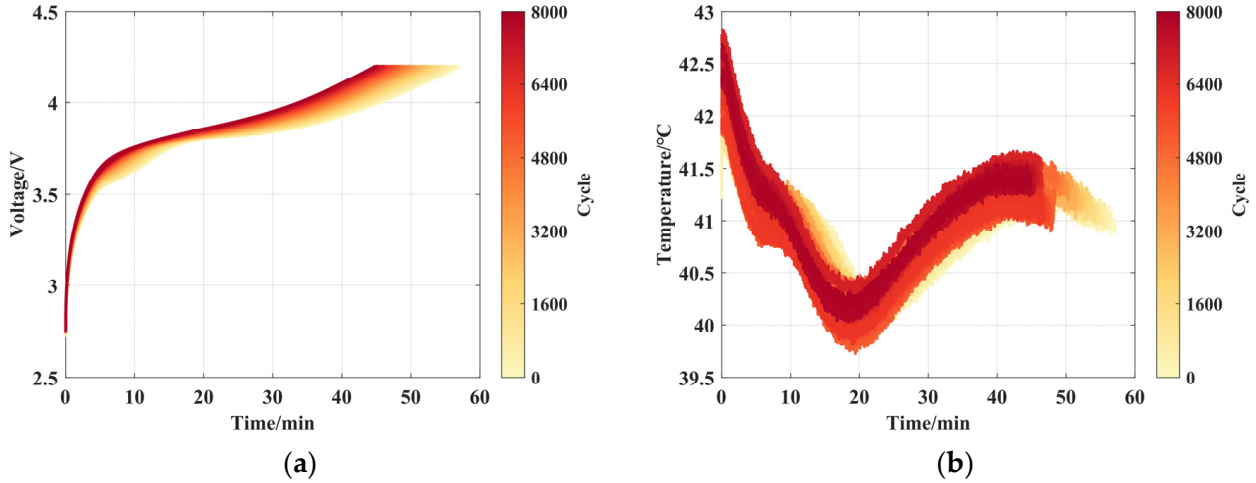

Figure 5. Charging voltage and temperature curve of Cell7. (**a**) Voltage. (**b**) Temperature.

3.2. Data Selection and Preprocessing

The Stanford–MIT–Toyota dataset experiences complex charging conditions, which exhibit richer characteristics of lithium-ion batteries than its smooth discharge process. The intuitive reflection of this can be observed through the voltage and temperature curve changes in Figure 4. Therefore, the complete charging voltage curve and temperature curve are selected to verify the RUL prediction method proposed in this study. The data selection of the Oxford dataset is also the same as the Stanford–MIT–Toyota dataset.

To ensure the data accurately reflect the battery aging characteristics and to facilitate the inspection of the RUL prediction method, data preprocessing is required. In the Stanford–MIT–Toyota dataset, there exists a small amount of outlier data that stems from occasional measuring instrument faults and periodic time information peaks during testing. These outliers cannot objectively reflect the nature of the battery itself and, therefore, require filtering. The Oxford dataset has had the anomalous cycle removed directly from the dataset before release.

Next, the data are resampled. During the cycle of the battery, the time elapsed in a series of charging curves obtained is different. For example, in the Stanford–MIT–Toyota dataset, the No. 11 battery spent 27 min on the first full charge, while the 761st charge took about 21 min. Hence, the number of data points is also different for each curve. To prevent the feature from biasing towards the charging curve with more data points, resampling is required so that each data sample has the same dimension. Since there is a certain error in the sampling time interval of the Stanford–MIT–Toyota dataset, an interpolation operation is performed first before resampling. In this way, the values of each charging curve can be aligned in time intervals. It is worth mentioning that the sampling interval of the Oxford dataset is stable at 1 s, so the interpolation process can be omitted. Afterward, resampling the charging curve can obtain a dataset with a uniform dimension.

Finally, the voltage and temperature variables in the charging curve are normalized, respectively. The method is as follows

$$x' = \frac{x - \min(x)}{\max(x) - \min(x)} \tag{20}$$

Since the voltage ranges and test temperature ranges of the batteries used in the two datasets are different, normalization should be performed within their respective value ranges to eliminate unnecessary errors caused by differences in the value ranges.

4. Experiment and Result Analysis

4.1. Evaluation Criteria

For the performance evaluation of the proposed approach, the mean absolute error (MAE), maximum error (MAX), root mean square error (RMSE) and mean absolute percentage error (MAPE) are selected. The equations are as follows:

$$\mathrm{MAE} = \frac{1}{n_c}\sum_{i=1}^{n_c}|y_i - \widetilde{y}_i| \tag{21}$$

$$\mathrm{MAX} = \max(|y_i - \widetilde{y}_i|) \tag{22}$$

$$\mathrm{RMSE} = \sqrt{\frac{1}{n_c}\sum_{i=1}^{n_c}(y_i - \widetilde{y}_i)^2} \tag{23}$$

$$\mathrm{MAPE} = \frac{1}{n_c}\sum_{i=1}^{n_c}\left|\frac{y_i - \widetilde{y}_i}{y_i}\right| \tag{24}$$

where the $\widetilde{y}_i$ and y_i are the predicted capacity and actual capacity for the lithium-ion battery, respectively. n_c represents the number of cycles when the battery reaches the EOL and i denotes the index of n_c. The lower these values, the more accurate the predicted results. In this study, computational time is also a pivotal evaluation criterion.

4.2. Implementation Details

The lithium-ion battery RUL prediction model established in Section 2 is verified with the two datasets preprocessed in Section 3. Specifically, transfer experiments of different working conditions and different types of batteries are designed. The former is to realize the RUL migration prediction capability between different working conditions on the same type of lithium-ion battery. The latter aims to realize the ability to migrate battery data from LFP to LCO. This subsection will introduce the dataset division and training way of these two experiments in detail.

4.2.1. Different Working Conditions

Table 2 shows the working conditions of each battery in the Stanford–MIT–Toyota dataset. To ensure that there are no overlapping working conditions between the source and target domains, the g2c32, g3c2, and g5c31 battery data each become the source domains, and some data in g1c38, g2c48, and g7c47 batteries are used as target domains. The data except for the target domains in g1c38, g2c48, and g7c47 are selected as the testing sets, respectively. The proportion of data volume is shown in Table 4.

Table 4. Dataset division and data size ratios in working conditions migration experiment.

Group		Source + Traget → Test	Data Volume Ratio
A	1	g5c31 + g1c38 → g1c38	1038:492:123
	2	g3c2 + g2c48 → g2c48	773:868:217
	3	g5c31 + g2c48 → g2c48	1038:868:217
	4	g2c32 + g7c47 → g7c47	988:591:147

4.2.2. Different Types of Batteries

The g1c38, g2c32, g2c48, g3c2, g5c31 and g7c47 battery data in the Stanford–MIT–Toyota dataset are used as the source domains. Part of the cell data of Cell1 and Cell7 in the Oxford dataset is used as the target domains. And select the Oxford dataset Cell1 and Cell7 battery data except for the target domains as the testing sets. Table 5 provides specific details.

Table 5. Dataset division and data size ratios in battery type migration experiment.

Group		Source + Traget → Test Dataset	Data Volume Ratio
B	1	g1c38 + Cell1 → Cell1	615:61:17
	2	g2c32 + Cell1 → Cell1	988:61:17
	3	g2c48 + Cell1 → Cell1	1085:61:17
	4	g3c2 + Cell1 → Cell1	773:61:17
	5	g5c31 + Cell1 → Cell1	1038:61:17
	6	g7c47 + Cell1 → Cell1	738:61:17
C	1	g1c38 + Cell7 → Cell7	615:59:17
	2	g2c32 + Cell7 → Cell7	988:59:17
	3	g2c48 + Cell7 → Cell7	1085:59:17
	4	g3c2 + Cell7 → Cell7	773:59:17
	5	g5c31 + Cell7 → Cell7	1038:59:17
	6	g7c47 + Cell7 → Cell7	738:59:17

4.2.3. Training Settings

To compare with the proposed RT-TrAdaBoost approach, experiments are also conducted on the more popular convolutional neural network transfer learning (CNN-TL) approach and the AdaBoost approach based on ensemble learning. The CNN-TL has a total of four one-dimensional convolutional layers, four pooling layers and one fully connected layer. The convolutional layer filters are 38, and the kernel size is 32. Both the AdaBoost approach and the RT-TrAdaBoost approach have 15 CART base learners, each with a maximum depth of 5 layers. In particular, as mentioned in Section 2.3, the AdaBoost approach assumes that all data available for training is identically distributed. Therefore, in the case that the target domain samples are insufficient to train the RUL prediction model alone, the target domain and source domain data are combined to train the AdaBoost.

4.3. Working Condition Migration Analysis

Table 4 in Section 4.2 divides the datasets used in the migration experiments. The experiments are conducted on Group A1, Group A2, Group A3 and Group A4. The RUL prediction results are shown in Figure 6.

From the experimental results in Figure 6, all approaches reflect the overall downward trend of lithium-ion battery RUL. However, there are differences between the three approaches. In the initial stage of RUL decline, the CNN-TL approach tends to exhibit significant prediction errors, whereas AdaBoost and RT-TrAdaBoost demonstrate superior fitting capabilities. In the middle stage of the battery cycle, the CNN-TL approach exhibits some fluctuations and is comparatively less robust than the other two boosting approaches. However, around the 100th and 400th cycles, fluctuations in the AdaBoost approach highlight the limitations of non-transfer learning methods to adapt to changing working conditions.

Figure 7 represents a more intuitive comparison of the error distribution between predicted and measured values. The yellow, pink and green parts represent the RUL prediction errors of the CNN-TL, AdaBoost and RT-TrAdaBoost, respectively. The error of the CNN-TL approach is much larger than that of AdaBoost and RT-TrAdaBoost, which confirms the prediction performance of the model in Figure 6. Further analysis shows that in GroupA1, GroupA3 and GroupA4, the RT-TrAdaBoost approach shows better performance than AdaBoost, the distribution of error data is more concentrated, and the error value is also smaller. But in GroupA2, the error performance of the RT-TrAdaBoost model is slightly worse than that of the AdaBoost approach, which may be caused by the fact that the sample size of the source domain in this group is smaller than that of the target domain. In the other three groups, the data size of source domains to battery aging migration is larger than that of the target domains. In comparison, the RT-TrAdaBoost model exhibits better predictive performance when a large number of historical samples are transferred to a smaller sample set.

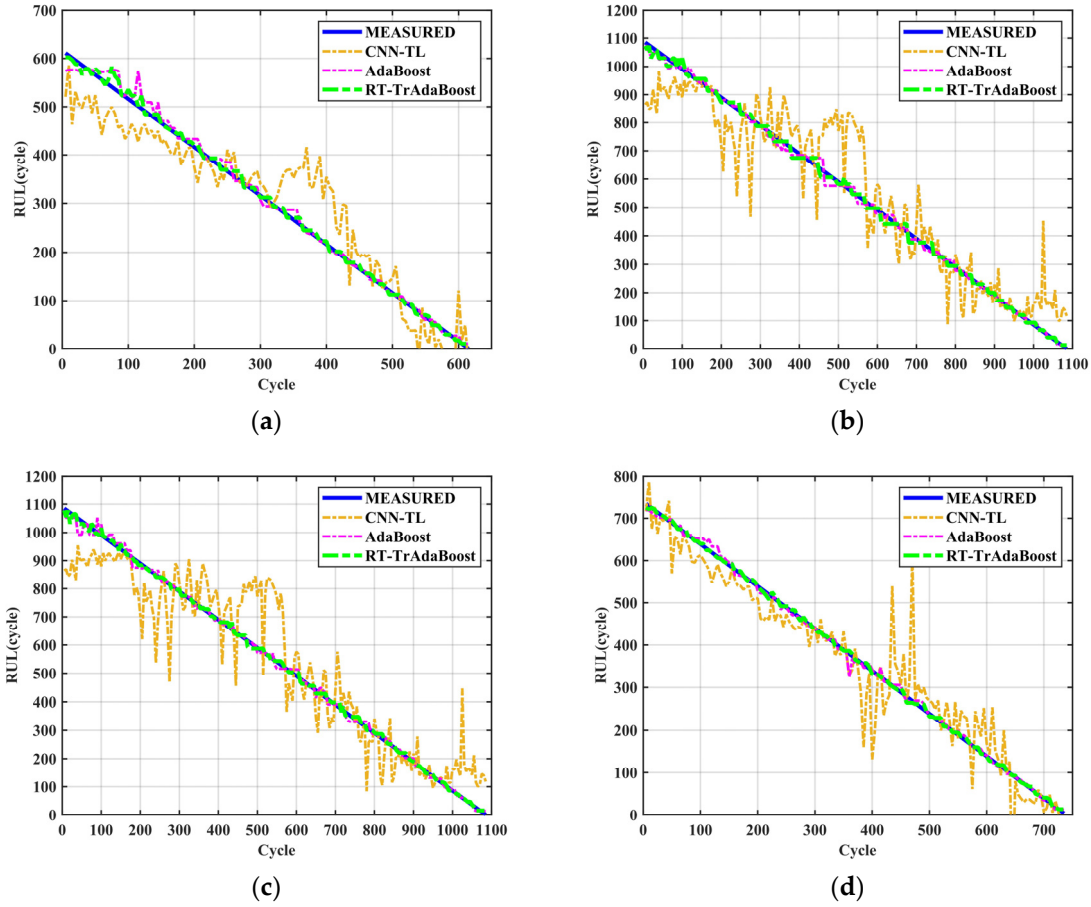

Figure 6. Lithium-ion battery RUL prediction results. (**a**) Transfer g5c31 to g1c38. (**b**) Transfer g3c2 to g2c48. (**c**) Transfer g5c31 to g2c48. (**d**) Transfer g2c32 to g7c47.

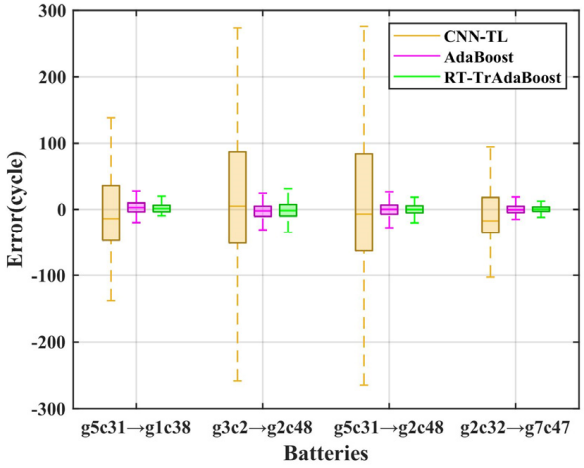

Figure 7. The error distribution of the different lithium-ion battery RUL prediction methods.

Figure 8 and Table 6 provide a comparative analysis of the evaluation results for each approach. The larger the criteria, the closer the color of the square approaches magenta; otherwise, it tends toward dark green. To highlight the differences in the evaluation criteria of each method in a single group, the color scale of each group is set independently. The MAE of the RT-TrAdaBoost model in the four groups reached 0.58%, 1.04%, 0.63% and 0.36%, respectively. The MAE of the AdaBoost algorithm is 0.91%, 0.99%, 0.94% and 0.58%. While the CNN-TL only performed 4.86%, 8.25%, 8.57% and 3.94%.

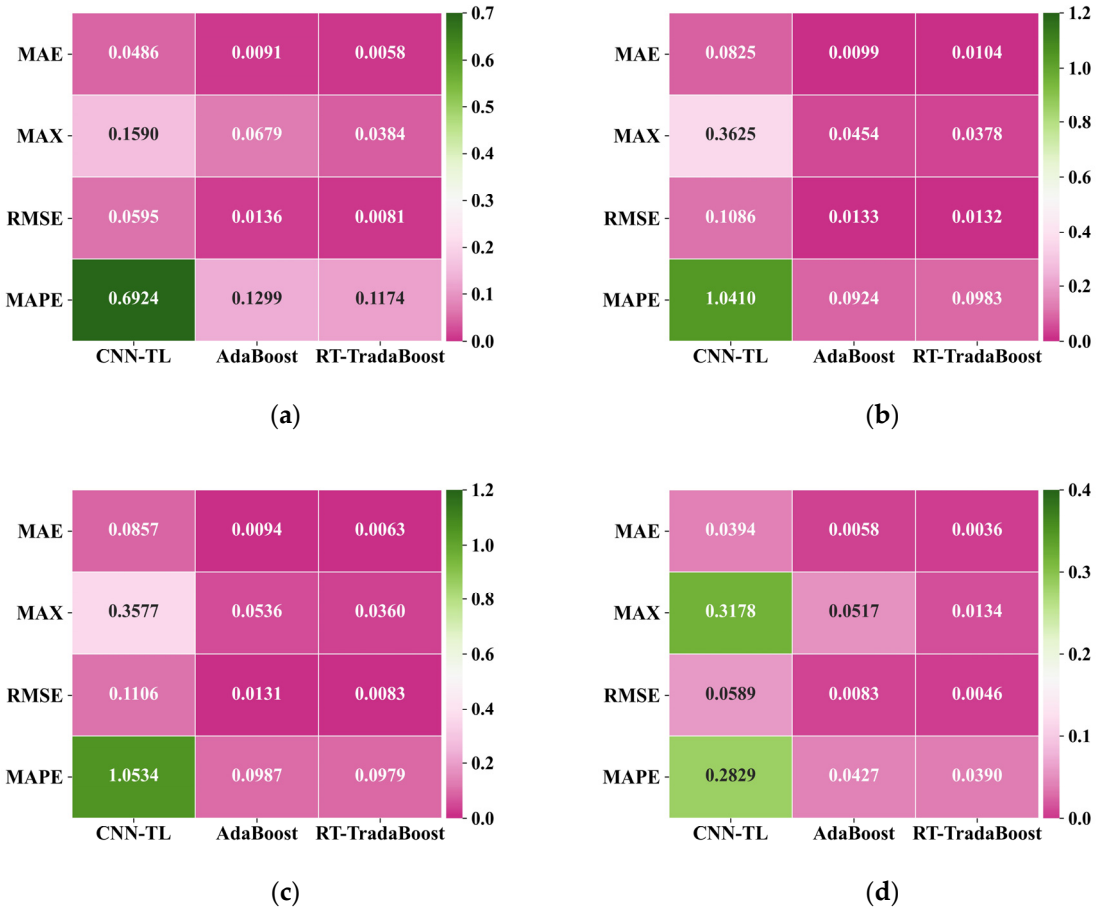

Figure 8. The evaluation criteria of lithium-ion battery RUL prediction results. (**a**) Transfer g5c31 to g1c38. (**b**) Transfer g3c2 to g2c48. (**c**) Transfer g5c31 to g2c48. (**d**) Transfer g2c32 to g7c47.

Table 6. The evaluation criteria of the working condition migration.

Group	Algorithms	MAE	MAX	RMSE	MAPE
A1	CNN-TL	0.0486	0.1590	0.0595	0.6924
	AdaBoost	0.0091	0.0679	0.0136	0.1299
	RT-TradaBoost	0.0058	0.0384	0.0081	0.1174
A2	CNN-TL	0.0825	0.3625	0.1086	1.0410
	AdaBoost	0.0099	0.0454	0.0133	0.0924
	RT-TradaBoost	0.0104	0.0378	0.0132	0.0983
A3	CNN-TL	0.0857	0.3577	0.1106	1.0534
	AdaBoost	0.0094	0.0536	0.0131	0.0987
	RT-TradaBoost	0.0063	0.0360	0.0083	0.0979
A4	CNN-TL	0.0394	0.3178	0.0589	0.2829
	AdaBoost	0.0058	0.0517	0.0083	0.0427
	RT-TradaBoost	0.0036	0.0134	0.0046	0.0390

Figures 7 and 8 jointly confirm the RUL prediction errors of the three methods. In addition to showing excellent performance in terms of average error, the RMSE of RT-TrAdaBoost is 0.81%, 1.32%, 0.83% and 0.46%, respectively. This means that there are almost no large outliers in the prediction results and reflects the robustness. From the color of the squares in Figure 8, the MAX and MAPE of the CNN-TL approach are much larger than the two ensemble learning methods. This shows that although the CNN-TL approach has a certain migration ability, it is still limited by the migration between different working conditions of the LFP battery. In summary, the RT-TrAdaBoost approach can efficiently

transfer aging knowledge from the source domain composed of historical data to the target domain on the target domain based on small samples. Although the charging conditions of these batteries are complex and varied, the method achieved satisfactory RUL prediction results in this experiment.

4.4. Battery Type Migration Analysis

After verifying the migration prediction effect of the RT-TrAdaBoost model in different working conditions, this paper further expands the migration prediction experiment between different types of batteries. In addition to the inconsistency of battery types, other factors, such as working conditions and temperature, also exhibit significant variations. This experiment will use six LFP batteries in the Stanford–MIT–Toyota dataset and two LCO batteries in the Oxford dataset, a total of 12 groups. As shown in Table 5, the sample size ratio of the source domain and the target domain in each group ranges from about 10:1 to 17.4:1. Similarly, the RUL prediction results on the three models are shown in Figures 9 and 10.

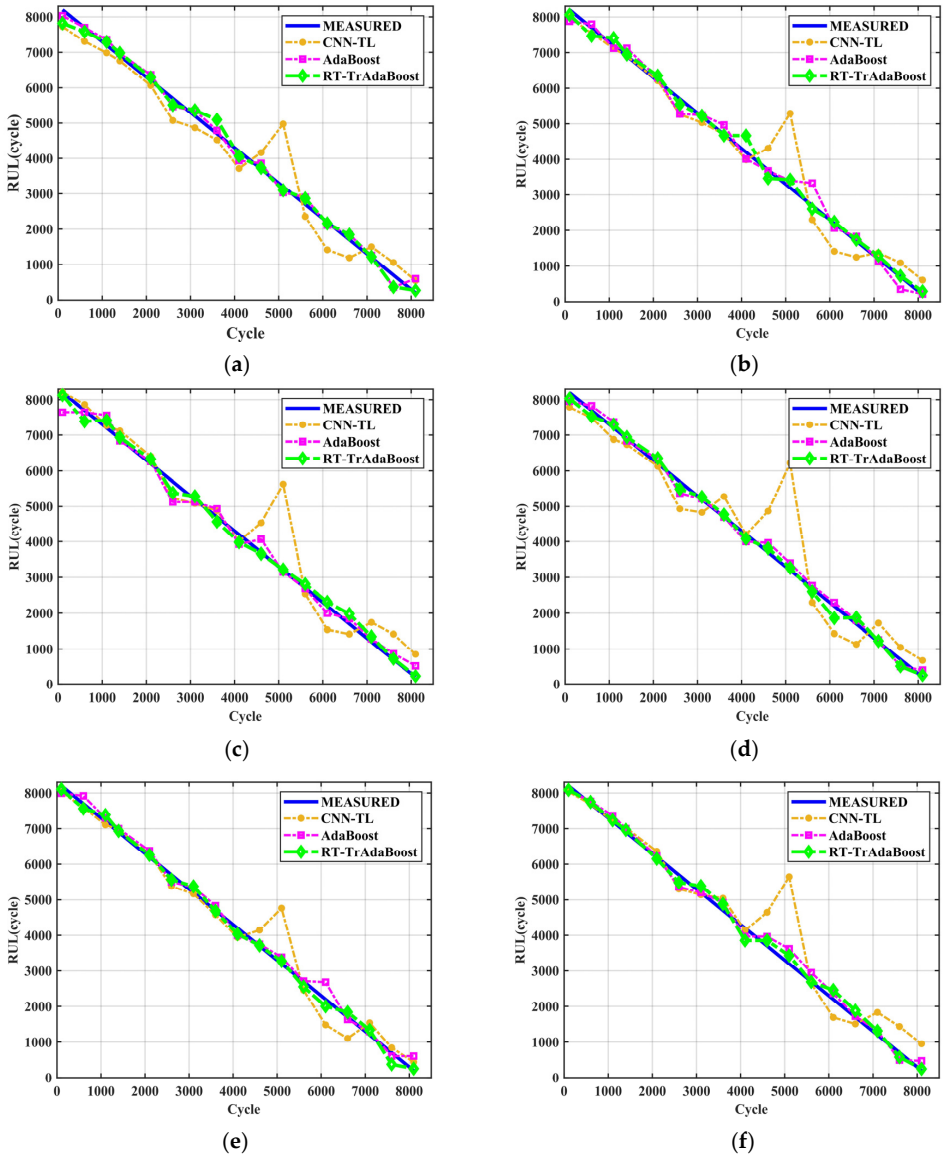

Figure 9. Transferable lithium-ion battery RUL prediction results from MIT–Stanford–Toyota dataset to Cell1. (**a**) g1c38. (**b**) g2c32. (**c**) g2c48. (**d**) g3c2. (**e**) g5c31. (**f**) g7c47.

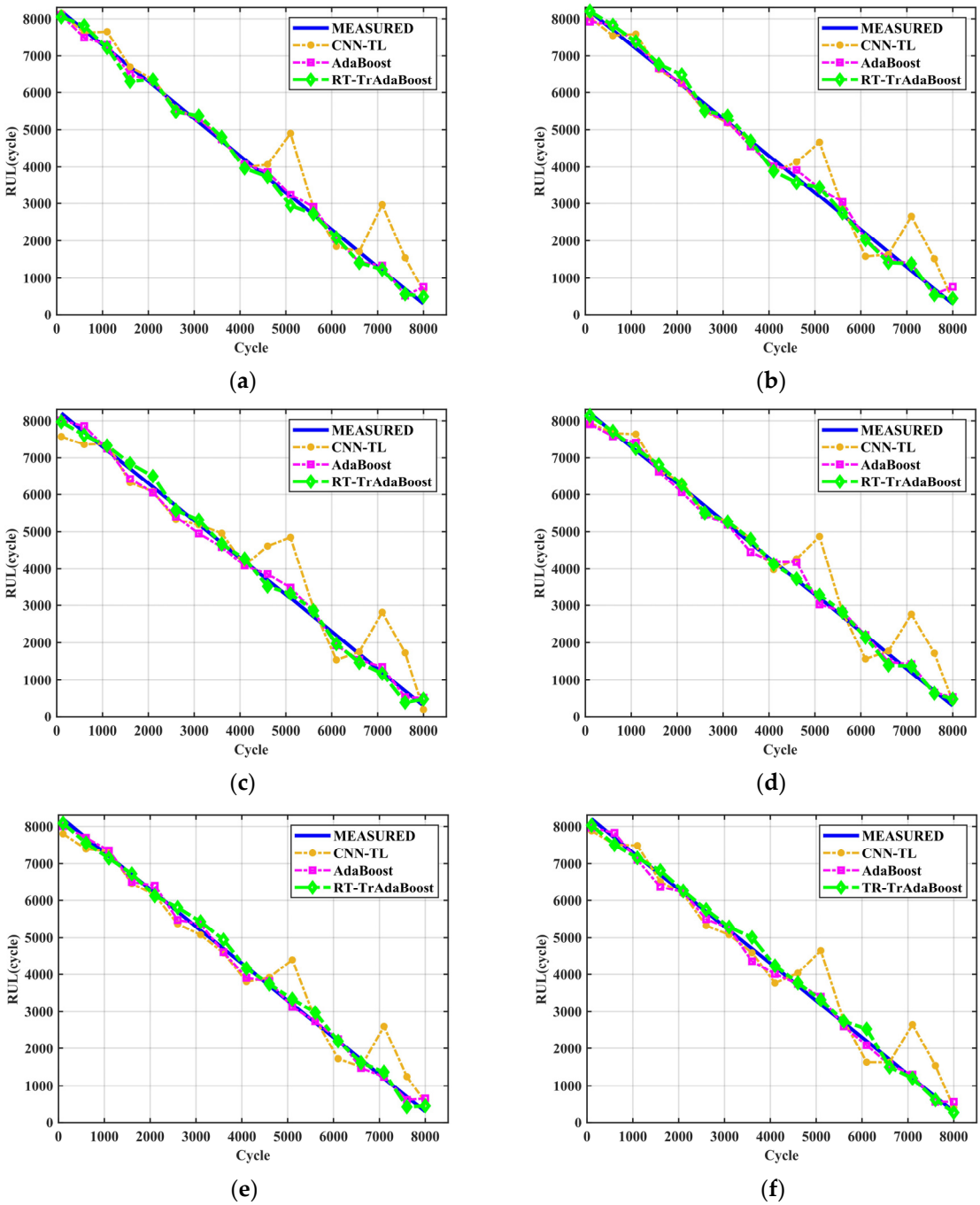

Figure 10. Transferable lithium-ion battery RUL prediction results from MIT–Stanford–Toyota dataset to Cell7. (**a**) g1c38. (**b**) g2c32. (**c**) g2c48. (**d**) g3c2. (**e**) g5c31. (**f**) g7c47.

In Figures 9 and 10, the RT-TrAdaBoost approach has excellent fitting performance and is more robust than the AdaBoost method. As for the CNN-TL, although the overall trend is consistent with the measured values, it exhibits fluctuations locally. Especially at the 4000th–7000th cycle, the fluctuation of the RUL prediction result curve is particularly severe. A similar situation also appears in Figure 10. However, although Cell1 and Cell7 are the same type of battery and their datasets are obtained under the same working condition, in contrast, the fluctuation of the CNN-TL approach in predicting Cell7 extends to around the 8000th cycle. This indicates that the CNN-TL also exhibits variances in its adaptability towards identical battery types, whereas the RT-TrAdaBoost approach is well-suited to address such discrepancies. By comparison, our proposed method has demonstrated

favorable RUL prediction outcomes across multiple batteries, showcasing both stability and precision.

From Figure 11, compared with the other two methods, the error distribution of the RT-TrAdaBoost method is more concentrated around 0. The finer model performance is reflected in Figures 12 and 13 through evaluation criteria. Tables 7 and 8 record the specific values. On the six batteries in Group B, the MAE of RUL prediction by the RT-TrAdaBoost method is 1.48% to 1.80%. In Group C, it ranges from 1.24% to 1.92%. The AdaBoost method and the CNN-TL approach are only 1.75% to 2.30% and 3.93% to 7.21% in Group B, respectively. In Group C, they are 1.78% to 2.24% and 4.64% to 6.13%, respectively. Regardless of the magnitude or scope of the error, it can be inferred that the RUL prediction outcome obtained through the RT-TrAdaBoost approach is more precise. From the evaluation of the RMSE index, for the Group B and Group C experiments, the RT-TrAdaBoost method is 1.50% to 2.24%, which is smaller than the AdaBoost method and the CNN-TL approach.

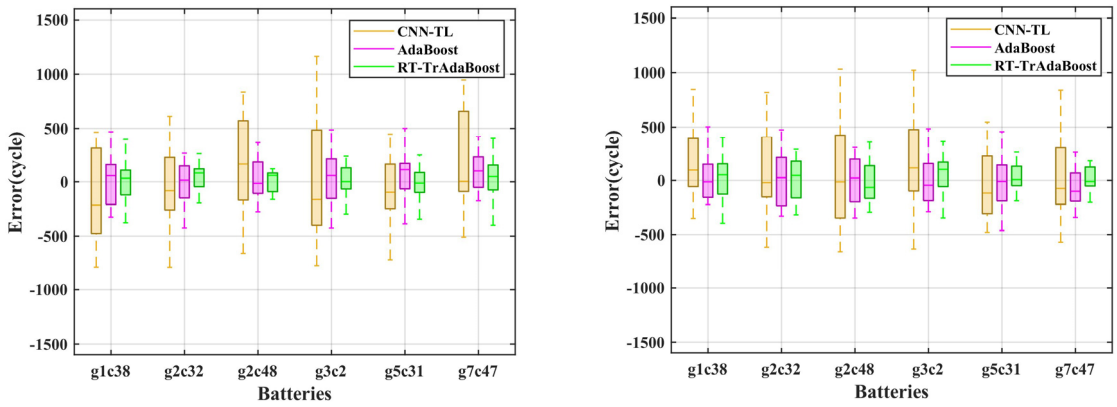

Figure 11. The error distribution of the results of different lithium-ion battery RUL prediction methods. (**a**) Cell1. (**b**) Cell7.

Table 7. The evaluation criteria of the battery type migration on Group B.

Group	Algorithms	MAE	MAX	RMSE	MAPE
B1	CNN-TL	0.0557	0.2137	0.0711	0.2620
	AdaBoost	0.0202	0.0482	0.0234	0.1798
	RT-TradaBoost	0.0180	0.0473	0.0224	0.0780
B2	CNN-TL	0.0466	0.2521	0.0740	0.2667
	AdaBoost	0.0233	0.0764	0.0302	0.0804
	RT-TradaBoost	0.0162	0.0560	0.0210	0.0604
B3	CNN-TL	0.0560	0.2932	0.0867	0.3830
	AdaBoost	0.0192	0.0538	0.0221	0.1070
	RT-TradaBoost	0.0162	0.0380	0.0201	0.0484
B4	CNN-TL	0.0721	0.3638	0.1077	0.3452
	AdaBoost	0.0175	0.0386	0.0204	0.1055
	RT-TradaBoost	0.0153	0.0408	0.0178	0.0640
B5	CNN-TL	0.0393	0.1884	0.0585	0.1921
	AdaBoost	0.0205	0.0580	0.0249	0.1664
	RT-TradaBoost	0.0148	0.0393	0.0175	0.0746
B6	CNN-TL	0.0538	0.2949	0.0879	0.4085
	AdaBoost	0.0212	0.0508	0.0252	0.1389
	RT-TradaBoost	0.0167	0.0417	0.0199	0.0637

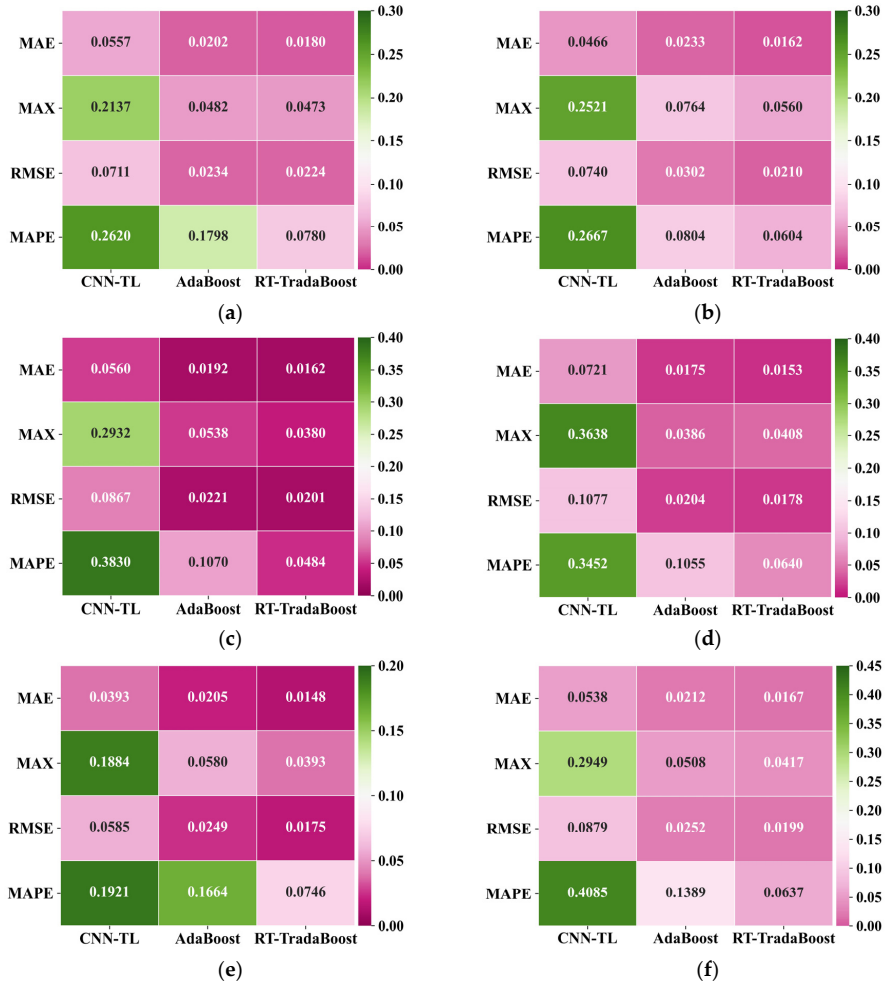

Figure 12. The evaluation criteria of lithium-ion battery RUL prediction results. (**a**) Transfer g1c38 to Cell1. (**b**) Transfer g2c32 to Cell1. (**c**) Transfer g2c48 to Cell1. (**d**) Transfer g3c2 to Cell1. (**e**) Transfer g5c31 to Cell1. (**f**) Transfer g7c47 to Cell1.

Table 8. The evaluation criteria of the battery type migration on Group C.

Group	Algorithms	MAE	MAX	RMSE	MAPE
C1	CNN-TL	0.0484	0.2127	0.0798	0.2894
	AdaBoost	0.0195	0.0551	0.0225	0.1440
	RT-TradaBoost	0.0187	0.0489	0.0223	0.0854
C2	CNN-TL	0.0464	0.1767	0.0712	0.2294
	AdaBoost	0.0217	0.0552	0.0251	0.1478
	RT-TradaBoost	0.0192	0.0384	0.0221	0.0870
C3	CNN-TL	0.0613	0.1987	0.0859	0.2773
	AdaBoost	0.0224	0.0357	0.0239	0.1036
	RT-TradaBoost	0.0188	0.0377	0.0211	0.0963
C4	CNN-TL	0.0521	0.2014	0.0797	0.2628
	AdaBoost	0.0204	0.0583	0.0249	0.0946
	RT-TradaBoost	0.0124	0.0361	0.0150	0.0733
C5	CNN-TL	0.0459	0.1685	0.0633	0.2326
	AdaBoost	0.0178	0.0427	0.0211	0.1074
	RT-TradaBoost	0.0154	0.0333	0.0185	0.0841
C6	CNN-TL	0.0491	0.1745	0.0713	0.2344
	AdaBoost	0.0193	0.0413	0.0223	0.0991
	RT-TradaBoost	0.0137	0.0396	0.0176	0.0424

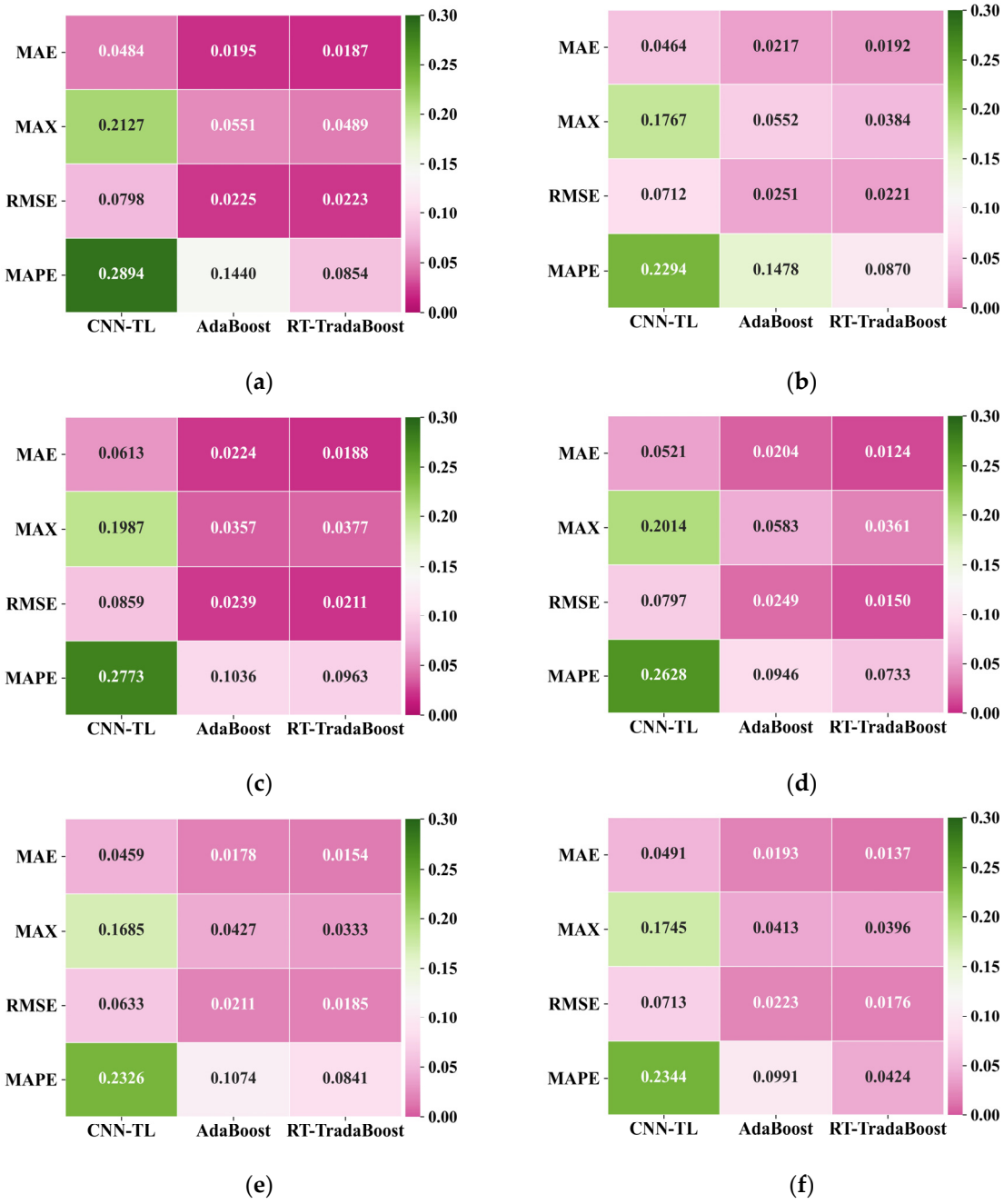

Figure 13. The evaluation criteria of lithium-ion battery RUL prediction results. (**a**) Transfer g1c38 to Cell7. (**b**) Transfer g2c32 to Cell7. (**c**) Transfer g2c48 to Cell7. (**d**) Transfer g3c2 to Cell7. (**e**) Transfer g5c31 to Cell7. (**f**) Transfer g7c47 to Cell7.

In addition, the color of the squares in Figures 12 and 13 highlights the large differences between the three models in the two evaluation criteria of MAX and MAPE. Therefore, on the Stanford–MIT–Toyota and Oxford datasets, the RT-TrAdaBoost method has an advantage in implementing aging information migration. Not only that but the operating conditions and temperatures of the two datasets are different. Therefore, under the joint action of multiple factors, the RUL prediction accuracy in the battery-type migration experiment is lower than that in the operating condition migration experiment, but the results still show that the model is effective. On the one hand, the utilization of historical battery data to migrate to a small sample of existing batteries for testing often encounters the challenge of being unable to match the battery type and charging conditions. The challenge has been effectively overcome in this experiment. On the other hand, the original

intention of choosing migration prediction is limited by the size of the battery data to be tested. This experiment still shows good predictive ability when the data scale ratio of the source domain and the target domain is set to nearly 17.4:1. In conclusion, the RT-TrAdaBoost method has a certain application value in RUL prediction.

4.5. Computational Efficiency Analysis

To show computing efficiency, we count the running time of the three methods on the personal computer and the edge computing module, respectively. Both model training and the first test are performed on a computer equipped with an AMD R7-4800H 2.90 GHz CPU, NVIDIA GeForce RTX 2060 (6GB on-board memory) GPU and 16GB RAM (3200 MHz). The second test is performed on an edge computing module known as the NVIDIA Jetson Xavier NX. Taking g1c38 migration to Cell1, for example, Table 9 records the average time of 10 runs.

Table 9. The runtime of lithium-ion battery RUL prediction methods.

Batteries	Time	CNN-TL	AdaBoost	RT-TrAdaBoost
g1c38 → Cell1	Training	241.77 s	7.776 s	10.33 s
	First testing	0.18 s	0.002 s	0.025 s
	Second testing	0.19 s	0.007 s	0.091 s

From Table 9, the CNN-TL approach with transfer learning ability requires a long training time. In contrast, both the AdaBoost method and the RT-TrAdaBoost model have shorter training times. In the two tests, the test times of the three models did not change in order of magnitude. The RT-TrAdaBoost takes much less time than the CNN-TL approach in both tests. Since the RT-TrAdaBoost has improved the weight distribution, it has performed certain operations in the process of transferring knowledge from the source domain to the target domain, so it takes slightly more time than the AdaBoost approach. However, considering the actual need to realize RUL prediction on BMS and comprehensively measure the time cost and prediction accuracy, the operation time of the RT-TrAdaBoost method is acceptable.

5. Conclusions

Accurate RUL prediction is especially important for reducing lithium-ion battery maintenance costs and improving equipment safety. This paper proposes a transferable RUL prediction approach based on small samples. The RT-TrAdaBoost model for RUL prediction we established not only overcomes the problem of a few battery aging data samples but also achieves transfer prediction between different working conditions and different types of batteries. The CART is chosen as the base learner improves the feature recognition ability of RT-TrAdaBoost. The well-characterized lithium-ion battery charge voltage and temperature curves are applied as input for RUL prediction. It has certain engineering practicability to mine useful information from BMS directly measurable data to predict RUL. Finally, the RT-TrAdaBoost model is deployed on computer and edge computing modules, and the accuracy and efficiency of the model are verified using two public datasets. The MAE and RMSE of transfer prediction under different working conditions ranged from 0.36% to 1.04% and 0.46% to 1.32%, respectively. In the migration experiment from LFP battery to LCO battery, the MAE and RMSE are 1.24% to 1.92% and 1.50% to 2.24%. Also, the values on MAX and MAPE are lower. In the future, there will be more comprehensive research conducted on the degradation of lithium-ion battery life, and data-driven methods will be explored to address issues such as dynamic perception and fault detection of lithium-ion battery aging. This paper can also provide ideas for the remaining life prediction of batteries made of other materials.

Author Contributions: Conceptualization, H.Q. and Y.F.; methodology, H.Q.; software, H.Q.; validation, H.Q., X.F. and Y.F.; formal analysis, Q.S.; investigation, R.W.; resources, D.Z.; data curation, H.Q.; writing—original draft preparation, H.Q.; writing—review and editing, Y.F.; visualization, H.Q.; supervision, X.F.; project administration, Y.F.; funding acquisition, Y.F. All authors have read and agreed to the published version of the manuscript.

Funding: This research was funded by the National Natural Science Foundation of China, grant number 52007196.

Institutional Review Board Statement: Not applicable.

Informed Consent Statement: Not applicable.

Data Availability Statement: Not applicable.

Conflicts of Interest: The authors declare no conflict of interest.

References

1. Tong, Z.; Miao, J.; Tong, S.; Lu, Y. Early Prediction of Remaining Useful Life for Lithium-Ion Batteries Based on a Hybrid Machine Learning Method. *J. Clean. Prod.* **2021**, *317*, 128265. [CrossRef]
2. Thelen, A.; Li, M.; Hu, C.; Bekyarova, E.; Kalinin, S.; Sanghadasa, M. Augmented Model-Based Framework for Battery Remaining Useful Life Prediction. *Appl. Energy* **2022**, *324*, 119624. [CrossRef]
3. Qin, P.; Zhao, L.; Liu, Z. State of Health Prediction for Lithium-Ion Battery Using a Gradient Boosting-Based Data-Driven Method. *J. Energy Storage* **2022**, *47*, 103644. [CrossRef]
4. Wang, Z.; Zeng, S.; Guo, J.; Qin, T. State of Health Estimation of Lithium-Ion Batteries Based on the Constant Voltage Charging Curve. *Energy* **2019**, *167*, 661–669. [CrossRef]
5. Wang, J.; Deng, Z.; Yu, T.; Yoshida, A.; Xu, L.; Guan, G.; Abudula, A. State of Health Estimation Based on Modified Gaussian Process Regression for Lithium-Ion Batteries. *J. Energy Storage* **2022**, *51*, 104512. [CrossRef]
6. Sangiri, J.B.; Kulshreshtha, T.; Ghosh, S.; Maiti, S.; Chakraborty, C. A Novel Methodology to Estimate the State-of-Health and Remaining-Useful-Life of a Li-Ion Battery Using Discrete Fourier Transformation. *J. Energy Storage* **2022**, *46*, 103849. [CrossRef]
7. Han, X.; Wang, Z.; Wei, Z. A Novel Approach for Health Management Online-Monitoring of Lithium-Ion Batteries Based on Model-Data Fusion. *Appl. Energy* **2021**, *302*, 117511. [CrossRef]
8. Zhang, Y.; Xiong, R.; He, H.; Pecht, M. Validation and Verification of a Hybrid Method for Remaining Useful Life Prediction of Lithium-Ion Batteries. *J. Clean. Prod.* **2019**, *212*, 240–249. [CrossRef]
9. *IEEE STd 1188-1996*; IEEE Recommended Practice for Maintenance, Testing, and Replacement of Valve-Regulated Lead-Acid (VRLA) Batteries for Stationary Applications. IEEE: New York, NY, USA, 1996.
10. Yang, H.; Wang, P.; An, Y.; Shi, C.; Sun, X.; Wang, K.; Zhang, X.; Wei, T.; Ma, Y. Remaining Useful Life Prediction Based on Denoising Technique and Deep Neural Network for Lithium-Ion Capacitors. *eTransportation* **2020**, *5*, 100078. [CrossRef]
11. Hu, X.; Xu, L.; Lin, X.; Pecht, M. Battery Lifetime Prognostics. *Joule* **2020**, *4*, 310–346. [CrossRef]
12. Hu, X.; Li, S.; Peng, H. A Comparative Study of Equivalent Circuit Models for Li-Ion Batteries. *J. Power Sources* **2012**, *198*, 359–367. [CrossRef]
13. Khodadadi Sadabadi, K.; Jin, X.; Rizzoni, G. Prediction of Remaining Useful Life for a Composite Electrode Lithium Ion Battery Cell Using an Electrochemical Model to Estimate the State of Health. *J. Power Sources* **2021**, *481*, 228861. [CrossRef]
14. An, D.; Choi, J.-H.; Kim, N.H. Prognostics 101: A Tutorial for Particle Filter-Based Prognostics Algorithm Using Matlab. *Reliab. Eng. Syst. Saf.* **2013**, *115*, 161–169. [CrossRef]
15. Ren, L.; Zhao, L.; Hong, S.; Zhao, S.; Wang, H.; Zhang, L. Remaining Useful Life Prediction for Lithium-Ion Battery: A Deep Learning Approach. *IEEE Access* **2018**, *6*, 50587–50598. [CrossRef]
16. Shen, S.; Sadoughi, M.; Li, M.; Wang, Z.; Hu, C. Deep Convolutional Neural Networks with Ensemble Learning and Transfer Learning for Capacity Estimation of Lithium-Ion Batteries. *Appl. Energy* **2020**, *260*, 114296. [CrossRef]
17. Kong, J.-Z.; Wang, D.; Yan, T.; Zhu, J.; Zhang, X. Accelerated Stress Factors Based Nonlinear Wiener Process Model for Lithium-Ion Battery Prognostics. *IEEE Trans. Ind. Electron.* **2022**, *69*, 11665–11674. [CrossRef]
18. Nagulapati, V.M.; Lee, H.; Jung, D.; Brigljevic, B.; Choi, Y.; Lim, H. Capacity Estimation of Batteries: Influence of Training Dataset Size and Diversity on Data Driven Prognostic Models. *Reliab. Eng. Syst. Saf.* **2021**, *216*, 108048. [CrossRef]
19. Wei, M.; Ye, M.; Wang, Q.; Xu, X.; Twajamahoro, J.P. Remaining Useful Life Prediction of Lithium-Ion Batteries Based on Stacked Autoencoder and Gaussian Mixture Regression. *J. Energy Storage* **2022**, *47*, 103558. [CrossRef]
20. Zhao, S.; Zhang, C.; Wang, Y. Lithium-Ion Battery Capacity and Remaining Useful Life Prediction Using Board Learning System and Long Short-Term Memory Neural Network. *J. Energy Storage* **2022**, *52*, 104901. [CrossRef]
21. Zhou, D.; Li, Z.; Zhu, J.; Zhang, H.; Hou, L. State of Health Monitoring and Remaining Useful Life Prediction of Lithium-Ion Batteries Based on Temporal Convolutional Network. *IEEE Access* **2020**, *8*, 53307–53320. [CrossRef]
22. Zhang, S.; Liu, Z.; Su, H. A Bayesian Mixture Neural Network for Remaining Useful Life Prediction of Lithium-Ion Batteries. *IEEE Trans. Transp. Electrif.* **2022**, *8*, 4708–4721. [CrossRef]

23. Zou, B.; Xiong, M.; Wang, H.; Ding, W.; Jiang, P.; Hua, W.; Zhang, Y.; Zhang, L.; Wang, W.; Tan, R. A Deep Learning Approach for State-of-Health Estimation of Lithium-Ion Batteries Based on a Multi-Feature and Attention Mechanism Collaboration. *Batteries* **2023**, *9*, 329. [CrossRef]
24. Sanz-Gorrachategui, I.; Pastor-Flores, P.; Pajovic, M.; Wang, Y.; Orlik, P.V.; Bernal-Ruiz, C.; Bono-Nuez, A.; Artal-Sevil, J.S. Remaining Useful Life Estimation for LFP Cells in Second-Life Applications. *IEEE Trans. Instrum. Meas.* **2021**, *70*, 2505810. [CrossRef]
25. Sagi, O.; Rokach, L. Ensemble Learning: A Survey. *WIREs Data Min. Knowl. Discov.* **2018**, *8*, e1249. [CrossRef]
26. Zhu, X.; Zhang, P.; Xie, M. A Joint Long Short-Term Memory and AdaBoost Regression Approach with Application to Remaining Useful Life Estimation. *Measurement* **2021**, *170*, 108707. [CrossRef]
27. Gao, L.; Kou, P.; Gao, F.; Guan, X. AdaBoost Regression Algorithm Based on Classification-Type Loss. In Proceedings of the 2010 8th World Congress on Intelligent Control and Automation, Jinan, China, 7–9 July 2010; pp. 682–687.
28. Finegan, D.P.; Zhu, J.; Feng, X.; Keyser, M.; Ulmefors, M.; Li, W.; Bazant, M.Z.; Cooper, S.J. The Application of Data-Driven Methods and Physics-Based Learning for Improving Battery Safety. *Joule* **2021**, *5*, 316–329. [CrossRef]
29. Birkl, C. Diagnosis and Prognosis of Degradation in Lithium-Ion Batteries. Ph.D. Thesis, University of Oxford, Oxford, UK, 2017.
30. Zhao, P.; Hoi, S.C.H. OTL: A Framework of Online Transfer Learning. In Proceedings of the 27th International Conference on Machine Learning (ICML-10), Haifa, Israel, 21–24 June 2010.
31. Pan, S.J.; Yang, Q. A Survey on Transfer Learning. *IEEE Trans. Knowl. Data Eng.* **2010**, *22*, 1345–1359. [CrossRef]
32. Wang, F.; Zhao, Z.; Ren, J.; Zhai, Z.; Wang, S.; Chen, X. A Transferable Lithium-Ion Battery Remaining Useful Life Prediction Method from Cycle-Consistency of Degradation Trend. *J. Power Sources* **2022**, *521*, 230975. [CrossRef]
33. Pan, D.; Li, H.; Wang, S. Transfer Learning-Based Hybrid Remaining Useful Life Prediction for Lithium-Ion Batteries Under Different Stresses. *IEEE Trans. Instrum. Meas.* **2022**, *71*, 3501810. [CrossRef]
34. Sun, X.; Liu, M.; Sima, Z. A Novel Cryptocurrency Price Trend Forecasting Model Based on LightGBM. *Financ. Res. Lett.* **2020**, *32*, 101084. [CrossRef]
35. Shi, M.; Hu, W.; Li, M.; Zhang, J.; Song, X.; Sun, W. Ensemble Regression Based on Polynomial Regression-Based Decision Tree and Its Application in the in-Situ Data of Tunnel Boring Machine. *Mech. Syst. Signal Process.* **2023**, *188*, 110022. [CrossRef]
36. Solomatine, D.P.; Shrestha, D.L. AdaBoost. RT: A Boosting Algorithm for Regression Problems. In Proceedings of the 2004 IEEE International Joint Conference on Neural Networks (IEEE Cat. No.04CH37541), Budapest, Hungary, 25–29 July 2004; Volume 2, pp. 1163–1168.
37. Attia, P.M.; Grover, A.; Jin, N.; Severson, K.A.; Markov, T.M.; Liao, Y.-H.; Chen, M.H.; Cheong, B.; Perkins, N.; Yang, Z.; et al. Closed-Loop Optimization of Fast-Charging Protocols for Batteries with Machine Learning. *Nature* **2020**, *578*, 397–402. [CrossRef] [PubMed]